Dirac points, new photonic band gaps, and effect of magnetically induced transparency in dichroic cholesteric liquid crystals with wavelength-dependent magneto-optical activity parameter

A. H. Gevorgyan ⬤

*Far Eastern Federal University, Institute of High Technologies and Advanced Materials, 10 Ajax Bay,
Russky Island, Vladivostok 690922, Russia*

We investigated the properties of cholesteric liquid crystals (CLCs) being in an external static magnetic field directed along the helix axis. We considered a dichroic CLC, that is, CLC with parameters $\mathrm{Re}\,\Delta = \frac{\mathrm{Re}\,\varepsilon_1 - \mathrm{Re}\,\varepsilon_2}{2} = 0$ and $\mathrm{Im}\,\Delta = \frac{\mathrm{Im}\,\varepsilon_1 - \mathrm{Im}\,\varepsilon_2}{2} \neq 0$, where $\varepsilon_{1,2}$ are the principal values of the local dielectric permittivity tensor. We have shown that in the case of the wavelength dependence of the magneto-optic activity parameter, new features appear in the optics of dichroic CLCs, in particular, in this case new Dirac points appear. Dirac points are points where there is an intersection of any two wave vector curves (they degenerate) and a linear law of the wave vector dependence on the frequency near these points. And moreover, at some Dirac points photonic band gaps (PBGs) appear; at others, lines of magnetically induced transparency (MIT), that is, a full transmission band appears, in an absorbing medium. In this case a polarization-sensitive transmission band appears too. At certain values of the helix pitch of the CLC and of the magnitude of the external magnetic field, three PBGs of different nature appear: a transmittance band, two narrow lines of MIT, and at others a broadband MIT, etc. This system is nonreciprocal, and the nonreciprocity changes over a wide range. It is observed both for reflection and transmittance and for absorption. The soft-matter nature of CLCs and their response to external influences lead to easily tunable multifunctional devices that can find a variety of applications. They can be applied as tunable narrow-band or broadband filters and mirrors, a highly tunable broad/narrow-band coherent perfect absorber, transmitter, ideal optical diode, and in other devices.

I. INTRODUCTION

Starting from pioneering papers by Yablonovich [1] and John [2], photonic crystals (PCs) are objects of intensive theoretical and experimental research, because the results of such investigations are finding more and more applications in photonic devices of the new generation. Some PCs exhibit novel mechanisms of some classical quantum effects, such as Bloch oscillations (oscillations of electrons within the Brillouin zone induced by an applied electric field) [1], Zener tunneling (the direct tunneling of a Bloch particle into a continuum of another energy band, which takes place without extra energy in the presence of a large electric field in the crystal) [2], electromagnetically induced transparency (EIT, which is a quantum interference effect in three-level atomic systems that eliminates the absorption at the resonance frequency and gives rise to a narrow transparency window) [3,4], electromagnetically induced absorption (EIA, which is the counterphenomenon of invoking constructive interference between multiple interaction pathways to enhance or induce absorption) [5], etc. In particular, some nanostructures in external magnetic fields or nanostructures with strong magnetic dipole interactions exhibit a narrow transparency window, and some others enhance or induce absorption. These new phenomena are called magnetically induced transparency (MIT) and magnetically induced absorption (MIA), respectively [6–15]. Magneto-optics of cholesteric liquid crystals (CLCs) is of particular interest. In this respect, they are also interesting because the

exact analytical solution of Maxwell's equation is known for the CLCs with magneto-optic activity (see [16]) and, consequently, clear and simple analytical formulas for the MIT and MIA frequencies can be obtained. The papers [16–26] present the results of a theoretical and experimental study of the magneto-optical properties of CLCs. Then, in the papers [27–30] the existence of MIT and MIA was demonstrated in the short-wavelength part of the spectrum in CLCs in the external magnetic field both at the presence and absence of local dielectric anisotropy. In [31] the observation of Dirac points in CLCs was reported, both in the presence of an external magnetic field and in its absence. It was shown that the MIT and MIA phenomena are observed exactly at the Dirac points.

However, all the works [16–31] deal with the case when the parameter of magneto-optical activity g is constant and is independent of wavelength. It was shown in [32] that in the case of the wavelength dependence of the magneto-optical activity parameter in the short-wavelength spectrum, no MIT effect nor MIA effect is observed. And now there is a natural question about the existence of these effects. These effects are to be expected because, as shown in [19], in the presence of an external magnetic field directed along the helix axis, two of the four wave vectors $k_m(\lambda)$ ($m = 1, 2, 3, 4$) are shifted upwards parallel to the axis $k_m = 0$ and the other two downwards. This means that for certain values of the medium's parameters and the external magnetic field, the wave vector curves may intersect and Dirac points may appear. Below we show that in the general case not only is their intersection possible

but also their practically exact coincidence in a quite wide frequency interval and the appearance of a Dirac line instead of a Dirac point. In this paper we analytically investigated the peculiarities of Dirac points and the unique properties of media near the Dirac points, and we investigated specific properties of the MIT effect in CLC in the limiting case in the absence of local birefringence and presence of local anisotropy of absorption, that is when $\text{Re}\Delta = \frac{\text{Re}\varepsilon_1 - \text{Re}\varepsilon_2}{2} = 0$ and $\text{Im}\Delta = \frac{\text{Im}\varepsilon_1 - \text{Im}\varepsilon_2}{2} \neq 0$, where $\varepsilon_{1,2}$ are the principal values of the local dielectric permittivity tensor. So we consider the case of dichroic CLC. In this paper we show the existence of new regions of the photonic band gaps (PBGs) and the Dirac points, and our consideration of this limiting case allows us to obtain simple analytical formulas for both for the boundaries of these PBGs and for the wavelengths of Dirac points, which with some accuracy can also be applied in the general case at $\text{Re}\Delta \neq 0$. Let us note that these formulas in the more general case of $\text{Re}\Delta \neq 0$ have more complex forms. This work is a sequential continuation of a number of already published articles [19–23,27–32] devoted to the magneto-optics of CLCs. Let us note that some features of the optical properties of dichroic CLCs are considered in detail in [33–35]. Moreover, the external magnetic field can also directly affect the local components of the dielectric tensor, being a new mechanism of local dielectric anisotropy, but since it is quadratic with respect to the external field effect, we can initially neglect it. Then the external magnetic field distorts the CLC structure, but since we are considering the case of CLC without local magnetic anisotropy, we can neglect this effect as well. Alternatively, at the end of the Conclusion section, we consider the case of CLC with local dielectric anisotropy and consider the effect of an external magnetic field on the pitch of the CLC helix and on the principal values of the components of the dielectric tensor.

II. MODELS AND METHODOLOGY. RESULTS

If the CLC is in an external magnetic field directed along the helix axis and the medium has a magneto-optical activity, then the tensors of dielectric permittivity and magnetic permeability will have the forms

$$\hat{\varepsilon}(z) = \varepsilon_m \begin{pmatrix} 1 + \delta\cos 2az & \pm\delta\sin 2az \pm ig/\varepsilon_m & 0 \\ \pm\delta\sin 2az \mp ig/\varepsilon_m & 1 - \delta\cos 2az & 0 \\ 0 & 0 & 1 - \delta \end{pmatrix}, \text{ and } \hat{\mu}(z) = \hat{I}, \tag{1}$$

where g is the parameter of magneto-optical activity of CLC, and it, in general, is a function of the external magnetic field, Verdet constant, and dielectric permittivity of media; $\varepsilon_m = (\varepsilon_1 + \varepsilon_2)/2$, $\delta = \frac{(\varepsilon_1 - \varepsilon_2)}{(\varepsilon_1 + \varepsilon_2)}$, $a = 2\pi/p$, where p is the pitch of the helix, and the axis z and external magnetic field are directed along the CLC helix axis. We take the dependence of g on wavelength as follows (see Appendix):

$$g = \frac{VB_{\text{ext}}\lambda}{\pi} \sqrt{\left| \varepsilon - \left(\frac{VB_{\text{ext}}\lambda}{2\pi}\right)^2 \right|}, \tag{2}$$

where V is the Verdet constant, and B_{ext} is the external magnetic field induction.

The dispersion equation now has the form

$$\left(\frac{\omega^2}{c^2}\varepsilon_1 - k_{mz}^2 - a^2\right)\left(\frac{\omega^2}{c^2}\varepsilon_2 - k_{mz}^2 - a^2\right)$$
$$- \left(2ak_{mz} - \frac{\omega^2}{c^2}g\right)^2 = 0. \tag{3}$$

As mentioned above, we will consider the limiting case, namely, the case of CLC in the absence of local birefringence, when $\text{Re}\Delta = \frac{\text{Re}\varepsilon_1 - \text{Re}\varepsilon_2}{2} = 0$ and $\text{Im}\Delta = \frac{\text{Im}\varepsilon_1 - \text{Im}\varepsilon_2}{2} \neq 0$, that is, we consider the case $\varepsilon_{1,2} = \varepsilon + i\varepsilon_{1,2}''$, where ε is the real part of the components of the dielectric constant tensor, which is assumed to be the same for all components. In this case Eq. (3) splits into two quadratic equations that have roots in the form

$$k_{1z} = \frac{\omega}{c}\sqrt{\varepsilon - g} + a, \quad k_{2z} = \frac{\omega}{c}\sqrt{\varepsilon + g} - a, \tag{4}$$

$$k_{3z} = -\frac{\omega}{c}\sqrt{\varepsilon - g} + a, \quad k_{4z} = -\frac{\omega}{c}\sqrt{\varepsilon + g} - a. \tag{5}$$

Figure 1 shows the dependence of g on wavelength λ. The function $g(\lambda)$ has two zeros on the wavelengths, $\lambda_1 = 0$ and $\lambda_2 = \frac{2\pi}{VB_{\text{ext}}}\sqrt{\varepsilon}$, and passes across local maximum on the wavelength $\lambda_3 = \frac{\pi}{VB_{\text{ext}}}\sqrt{2\varepsilon}$.

Substituting $\lambda_3 = \frac{\pi}{VB_{\text{ext}}}\sqrt{2\varepsilon}$ into (2) for g at the wavelength λ_3, we will have g $= \varepsilon$. From (4) it follows that at this wavelength we will have $k_{1z} = k_{3z}$, that is, they degenerate. Taking into account the approximately linear dependence of k_{iz} onto frequency ω near the wavelength λ_3, here at the wavelength λ_3 we have the Dirac point, and here the touching of the vertices of the Dirac cones takes place. We now investigate the optical properties of dichroic CLCs near these points.

Figure 2 shows the dependences of real and imaginary parts of wave vectors k_{iz} on wavelength λ. As can be seen from these graphs, there is one more characteristic
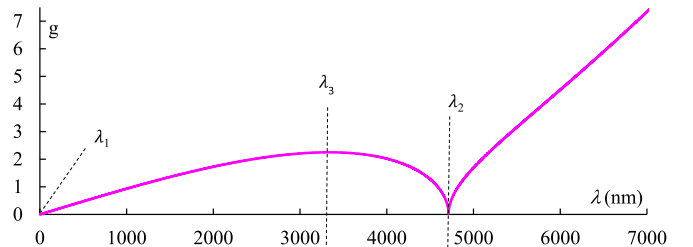
FIG. 1. The dependence of g on wavelength λ. The parameters are $\varepsilon = 2.25$, $V = \text{const} = 5 \times 10^5$ rad/(T m), $B_{\text{ext}} = 40$ T.
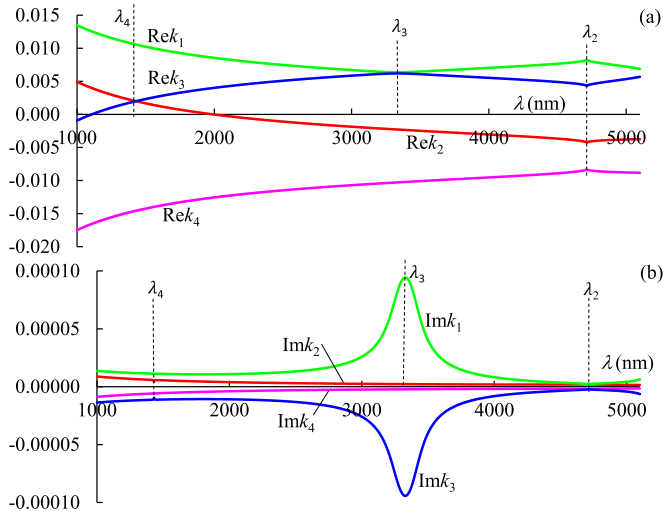
FIG. 2. The dependences of (a) real and (b) imaginary parts of wave vectors k_{iz} on wavelength λ: $p = 1000$ nm, $\mathrm{Im}\varepsilon_1 = 0.01$, and $\mathrm{Im}\varepsilon_2 = 0$. The other parameters are the same as in Fig. 1.

FIG. 3. The spectra of reflection R (curves 1 and 2), transmission T (curves 3 and 4), and absorption A (curves 5 and 6) at different directions of external magnetic field. The incident light has polarization coinciding with the first EP (curves 1, 3, 5) and with the second EP (curves 2, 4, 6). (a) The directions of the incident light and the external magnetic field coincide and (b) they are oppositely directed. CLC layer thickness $d = 50p$. The other parameters are the same as in Fig. 2.

wavelength, namely, λ_4, where the intersection of curves $\mathrm{Re}k_{2z}(\lambda)$ and $\mathrm{Re}k_{3z}(\lambda)$ occurs, that is, now, at this wavelength, k_{2z} and k_{3z} degenerate. Again, taking into account the approximately linear dependence of k_{iz} on frequency ω near the wavelength λ_4, here at wavelength λ_4 again we have the Dirac point. By equating k_{2z} to k_{3z} from (4) and taking into account (2) we obtain the expression for the wavelength for this Dirac point: $\lambda_4 = 2\pi p\sqrt{\frac{\varepsilon}{4\pi^2+V^2\,B_{\mathrm{ext}}^2\,p^2}}$. At the presence of anisotropic absorption ($Re\varepsilon_1 = Re\varepsilon_2 = \varepsilon$, but $Im\varepsilon_1 \neq Im\varepsilon_2$) a PBG is formed here, which exists also at the absence of external magnetic field.

Now, using the exact analytical solution of the Maxwell's equations for magnetoactive CLC [16] and the dispersion equation (3), we can solve the problem of light reflection, transmission, and absorption in the case of a planar magnetoactive CLC layer of finite thickness. We assume that the optical axis of this CLC layer is perpendicular to the boundaries of the layer and is directed along the z axis. The CLC layer has a border on both sides with isotropic half-spaces with the same refractive indices equal to n_s. The boundary conditions, consisting of the continuity of the tangential components of the electric and magnetic fields, are a system of eight linear equations with eight unknowns (for more detail see [16]). Solving this boundary-value problem, one can determine the values of the reflected $\mathbf{E}_r$ and transmitted $\mathbf{E}_t$ fields and calculate the energy coefficient of reflection $R = \frac{|\mathbf{E}_r|^2}{|\mathbf{E}_i|^2}$, transmission $T = \frac{|\mathbf{E}_t|^2}{|\mathbf{E}_i|^2}$, and absorption $A = 1 - (R + T)$, where $\mathbf{E}_i$ is the incident light field. Here and below we consider the case of minimal influence of dielectric boundaries, that is, the case $n_s = \sqrt{\varepsilon_m}$.

Figure 3 shows the spectra of reflection R (curves 1 and 2), transmission T (curves 3 and 4), and absorption A (curves 5 and 6) at different directions of external magnetic field. The incident light has polarization coinciding with the first eigenpolarization (EP) (curves 1,3,5) and with the second EP (curves 2, 4,6). In Fig. 3(a) the directions of the incident light and the external magnetic field coincide, and in Fig. 3(b)
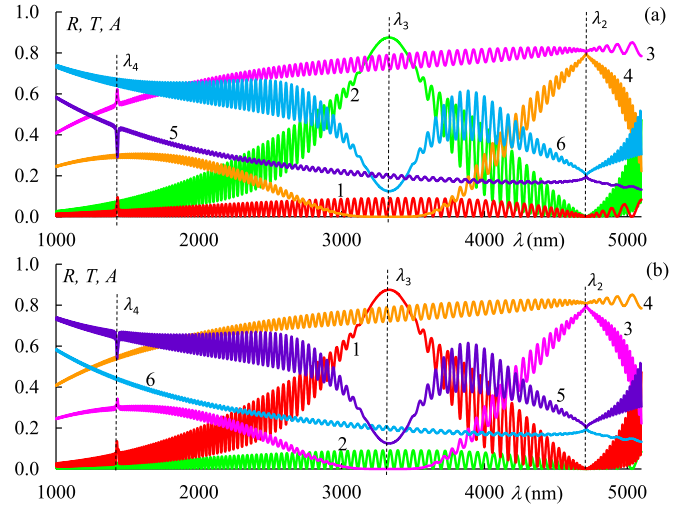
they are oppositely directed. By definition, the EPs are the two polarizations of incident light that do not change as the light passes through the system. These two EPs for dichroic CLC approximately coincide with orthogonal circular polarizations. Some discrepancy arises only near the wavelength λ_2. The helix of our CLC is right-handed. Let us now enumerate the EPs in the following way. We will assume that the first EP is the EP that approximately coincides with the right-hand circular polarization while the second EP coincides with the left-hand one.

As can be seen from Fig. 3, in the Dirac point at the wavelength λ_4, diffraction reflection undergoes light with a polarization coinciding with the first EP. This PBG exists also at the absence of external magnetic field, and in this case $\lambda_4 = p\sqrt{\varepsilon}$. At the presence of local birefringence there arises a PBG with a finite frequency width with $\Delta\lambda = p\Delta n = p(\sqrt{Re\varepsilon_1} - \sqrt{Re\varepsilon_2})$. Once again, let us note that the PBG arising in this case is determined by the structure of the CLC, i.e., the chirality sign of the polarization of the incident diffracting light is determined only by the chirality sign of the CLC helix. We call this PBG the first (or basic) PBG.

A new PBG is formed in the Dirac point near the wavelength λ_3. We call this PBG the second PBG. This new PBG is sensitive to the polarization of the incident light too. The chirality sign of the polarization of the incident diffracting light for the first PBG is determined only by the chirality sign of the CLC helix, while for the second one it is determined by the external magnetic field direction (i.e., on whether the directions of the external magnetic field and the incident light are parallel, or they are antiparallel). In the first case, the diffraction reflection undergoes the light with the second EP, and in the second case, the light with the first EP.

Near the wavelength λ_2 a transmission band is formed for incident light with a certain polarization. And as for the
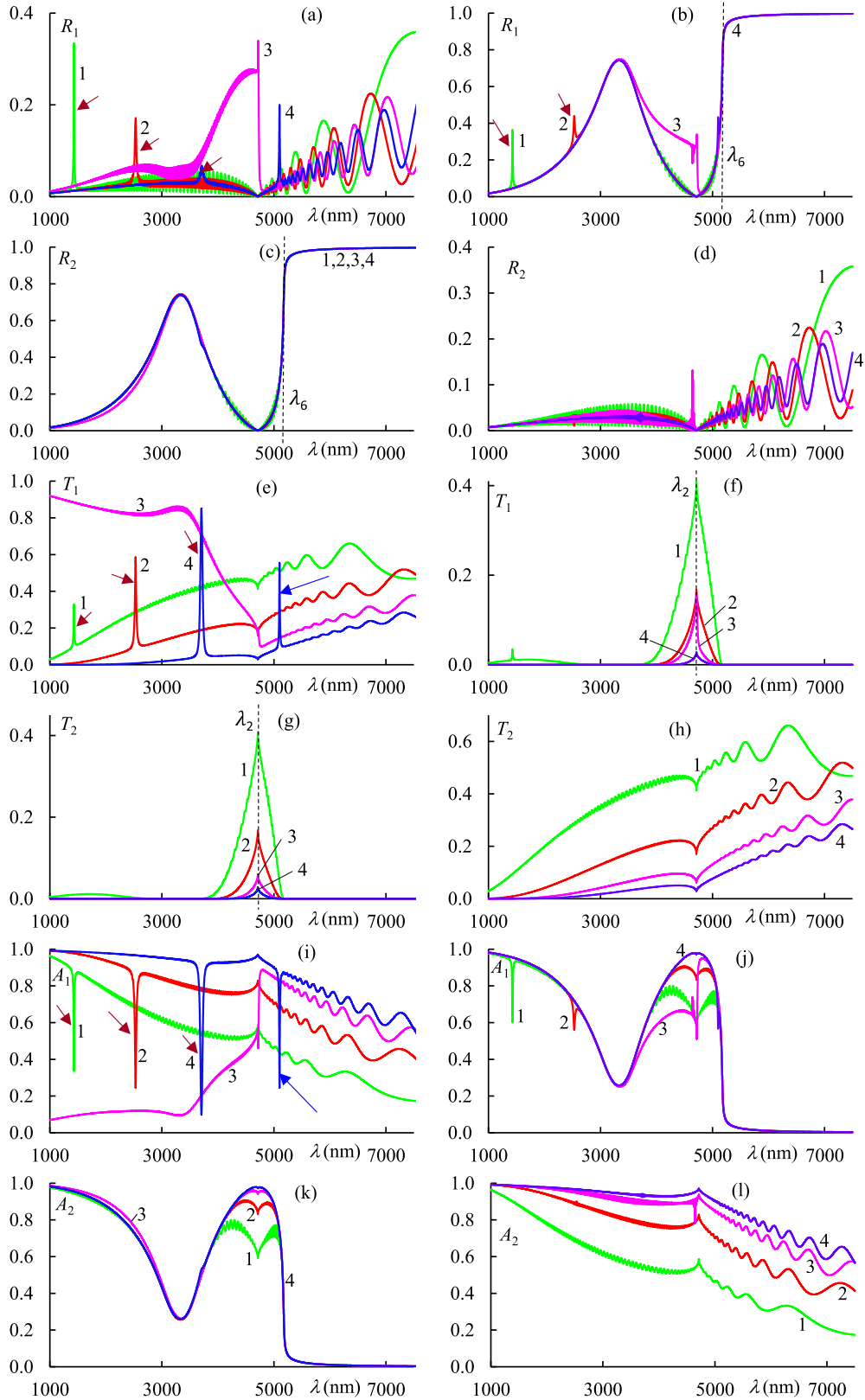
FIG. 4. The spectra of reflection, transmission, and absorption at different values of helix pitch. The incident light has polarization coinciding with the first EP (R_1, T_1, A_1) and with the second EP (R_2, T_2, A_2). In (a, c, e, g, i, k) the directions of the incident light and the external magnetic field coincide, while in (b, d, f, h, j, l) they are oppositely directed. $p = 1000$ nm (curves 1), $p = 2000$ nm (curves 2), $p = 3150$ nm (curves 3), and finally, $p = 4000$ nm (curves 4). $\mathrm{Im}\varepsilon_1 = 0.05$, $\mathrm{Im}\varepsilon_2 = 0$, $d = 50p$. The other parameters are the same as in Fig. 2.

second PBG, the chirality sign of the polarization of the incident light for which transmission bands were formed is determined by the external magnetic field direction. Let us note another unique property of chiral CLCs at the λ_2 wavelength itself. At this wavelength, reflection, transmittance, and absorption are independent of the polarization of the incident wave.

The reflection, transmission, and absorption spectra at different values of helix pitch are shown in Fig. 4. The incident light has polarization coinciding with the first EP (R_1, T_1, A_1) and with the second EP (R_2, T_2, A_2). In Figs. 4(a), 4(c), 4(e), 4(g), 4(i), and 4(k), the directions of the incident light and the external magnetic field coincide, while in Figs. 4(b), 4(d), 4(f), 4(h), 4(j), and 4(l) they are oppositely directed.

From the presented spectra, the following is observed:

(1) This system is nonreciprocal. In Fig. 4 the spectra in the left column differ significantly from those in the right column, and the nonreciprocity changes over a wide range. it is observed both for reflection and transmittance, and for absorption.

(2) With an increase in the pitch of the helix, the height of the peaks of reflection of the first PBG decreases [in Figs. 4(a) and 4(b), these peaks are highlighted by brown arrows].

(3) At the given parameters of the problem, in the region $\lambda \geqslant \lambda_6 = 5180$ nm (about λ_6 see below) a new PBG (the third PBG) is formed that is sensitive to the polarization of the incident light [see Figs. 4(b) and 4(c)].

(4) With an increase in the pitch of the helix, the height of the peaks of transmission of the first PBG on the wavelength λ_4 increases for the first EP [in Fig. 4(e) these peaks are highlighted by brown arrows]. Simultaneously, an increase in the height of the dips in the absorption on this wavelength for the first EP takes place too [in Fig. 4(i) these dips are highlighted by brown arrows], and as noted above in point (2), there is a decrease in the height of the reflection peaks on this wavelength. Thus we have the following picture: With an increase in the pitch of the helix, the PBG at wavelength λ_4 gradually turns into a narrow window of MIT, i.e., in the Dirac point at this wavelength, for some parameters of the problem, diffraction reflection is observed, and for others, a narrow window of MIT with a continuous transition from one state to another.

(5) With an increase in the pitch of the helix, the height of the peaks of the transmission band near the wavelength λ_2 decreases [see Figs. 4(f) and 4(g)].

(6) At a certain value of the helix pitch, instead of a narrow line of magneto-induced transmission, a broadband region of magneto-induced transmission is formed [see Figs. 4(e) and 4(i), curve 3]. As our calculations show, at these parameters, here in a wide enough wavelength band, we have $k_{1z} = k_{2z}$, and a Dirac line instead of a Dirac point appears. At the presence of anisotropic absorption here, unidirectional transmission takes place, and this system can work as a wideband, practically ideal optical diode.

(7) At certain values of the external magnetic field and helix pitch, a new Dirac point appears and a new MIT line is observed in the spectra [indicated by a blue arrow in Figs. 4(e) and 4(i)]. As our calculations show, there is a new Dirac point here. It appears due to the intersection of the curves $\mathrm{Re}k_{1z}(\lambda)$ and $\mathrm{Re}k_{2z}(\lambda)$. By equating k_{1z} to k_{2z} from (4) and taking into
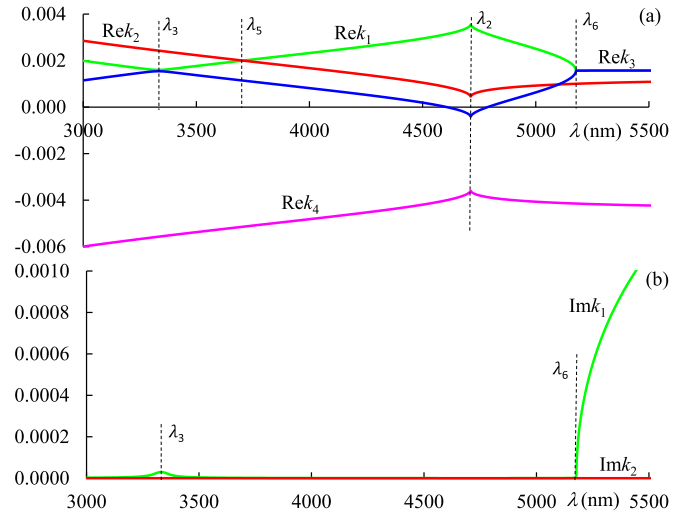
FIG. 5. The dependences of (a) real and (b) imaginary parts of wave vectors k_{iz} on wavelength λ. $p = 4000$ nm, $\mathrm{Im}\varepsilon_1 = 0.0001$, $\mathrm{Im}\varepsilon_2 = 0$. The other parameters are the same as in Fig. 1.

account (2), we obtain the expression for the wavelength for this Dirac point: $\lambda_5 = 2\pi p\sqrt{\frac{\varepsilon(4\pi^2 + V^2 B_{\mathrm{ext}}^2 p^2)}{16\pi^4 + V^4 B_{\mathrm{ext}}^4 p^4}}$. Figure 5 shows the dependences of real and imaginary parts of wave vectors k_{iz} on wavelength λ in the situation where there is an intersection of curves $\mathrm{Re}k_{1z}(\lambda)$ and $\mathrm{Re}k_{2z}(\lambda)$.

(8) As follows from (4), at $\mathrm{g} \geqslant \varepsilon$ two from four wave vectors become complex at the absence of absorption and a new (the third) PBG appears. From condition $\mathrm{g} = \varepsilon$ we obtain two wavelengths, namely, $\lambda_3 = \frac{\pi}{VB_{\mathrm{ext}}}\sqrt{2\varepsilon}$ and $\lambda_6 = \frac{\pi\sqrt{2\varepsilon}}{VB_{\mathrm{ext}}}\sqrt{1 + \sqrt{2}}$. As mentioned above, at the local maximum of $\mathrm{g}(\lambda)$ we have $\mathrm{g} = \varepsilon$, too.

Now we will investigate the evolution of spectra of reflection, transmission, and absorption at the change of helix pitch p and of B_{ext}, for the most complete representation of the features of these spectral changes when changing the helix pitch and external static magnetic field.

Figure 6 shows the evolution of the spectra of (a, b) reflection R, (c, d) transmission T, and (e, f) absorption A at the change of the helix pitch. The incident light has polarization coinciding with the first EP (left column) and with the second EP (right column). The directions of the incident light and the external magnetic field coincide.

These evolutions demonstrate the independence of the wavelengths determining the boundaries of the second and third PBGs, as well as the transmission band near wavelength λ_2, from the pitch of the helix. This is expressed in the appearance of horizontal bands of red or blue in the spectra of reflection, transmission, and absorption for incident light with polarization coinciding with the second EP. Of course, this also follows directly from the formulas for the wavelengths λ_3, λ_6, and λ_2, presented above. In Fig. 6(b) these areas are highlighted by white arrows. Further, Figs. 6(a), 6(c), and 6(e) demonstrate the transformation of the region of the first PBG into a narrow window of MIT with an increase in the pitch of the helix. Figures 6(c)–6(f) demonstrate two more interesting effects (see also above), namely, at a helix pitch
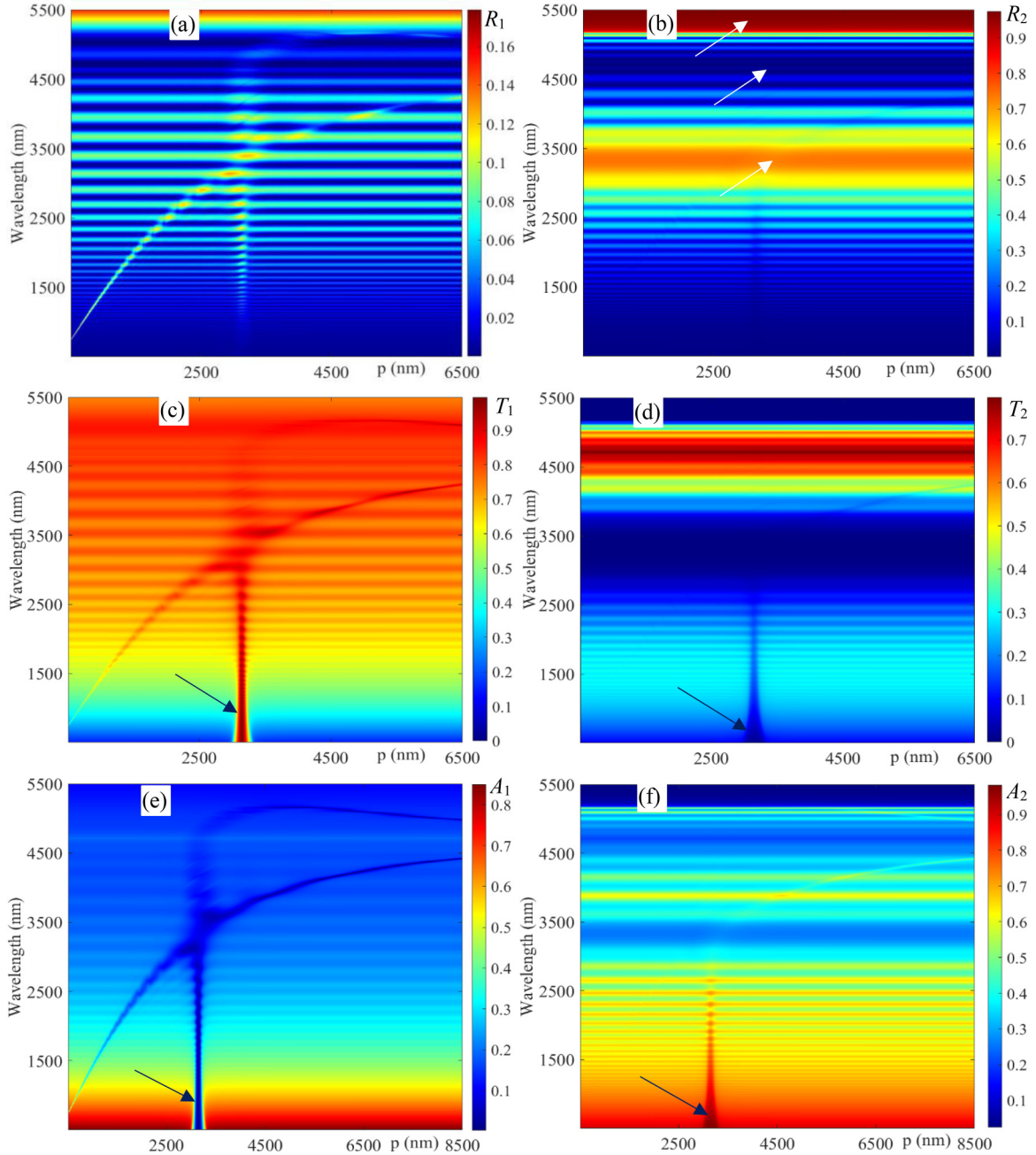
FIG. 6. The evolution of the spectra of (a, b) reflection R, (c, d) transmission T, and (e, f) absorption A for various values at the change of the helix pitch. The incident light has polarization coinciding with the first EP (left column) and with the second EP (right column). The directions of the incident light and the external magnetic field coincide; $d = 20p$. The other parameters are the same as in Fig. 4.

of about 3150 nm, a broadband region of MIT is formed for the mode with the first EP [Figs. 6(c) and 6(e)] and a region of MIA for the mode with the second EP [Figs. 6(d) and 6(f)]. They are highlighted by black arrows. As mentioned above, here we have a Dirac line. In the first case, a coherent perfect transmission occurs in a significantly broadband region, and in the second case, a coherent perfect absorption occurs, again in a broadband region. In this region, for the first EP we have wideband coherent perfect transmission (transmission of about 100%), and here ideal unidirectional transmission takes place, too. That is, here this CLC layer can

work as a tunable ideal optical diode. For the second EP here, a wideband coherent absorption takes place (absorption of about 100%).

And finally, Fig. 7 shows the evolution of the spectra of (a, b) reflection R, (c, d) transmission T, and (e, f) absorption A at the change of external magnetic field. The incident light has polarization coinciding with the first EP (left column) and with the second EP (right column). Here, $B = B_{ext} > 0$ means that the direction of light propagation and the direction of the external magnetic coincide, while $B_{ext} < 0$ means that these directions are reverse.
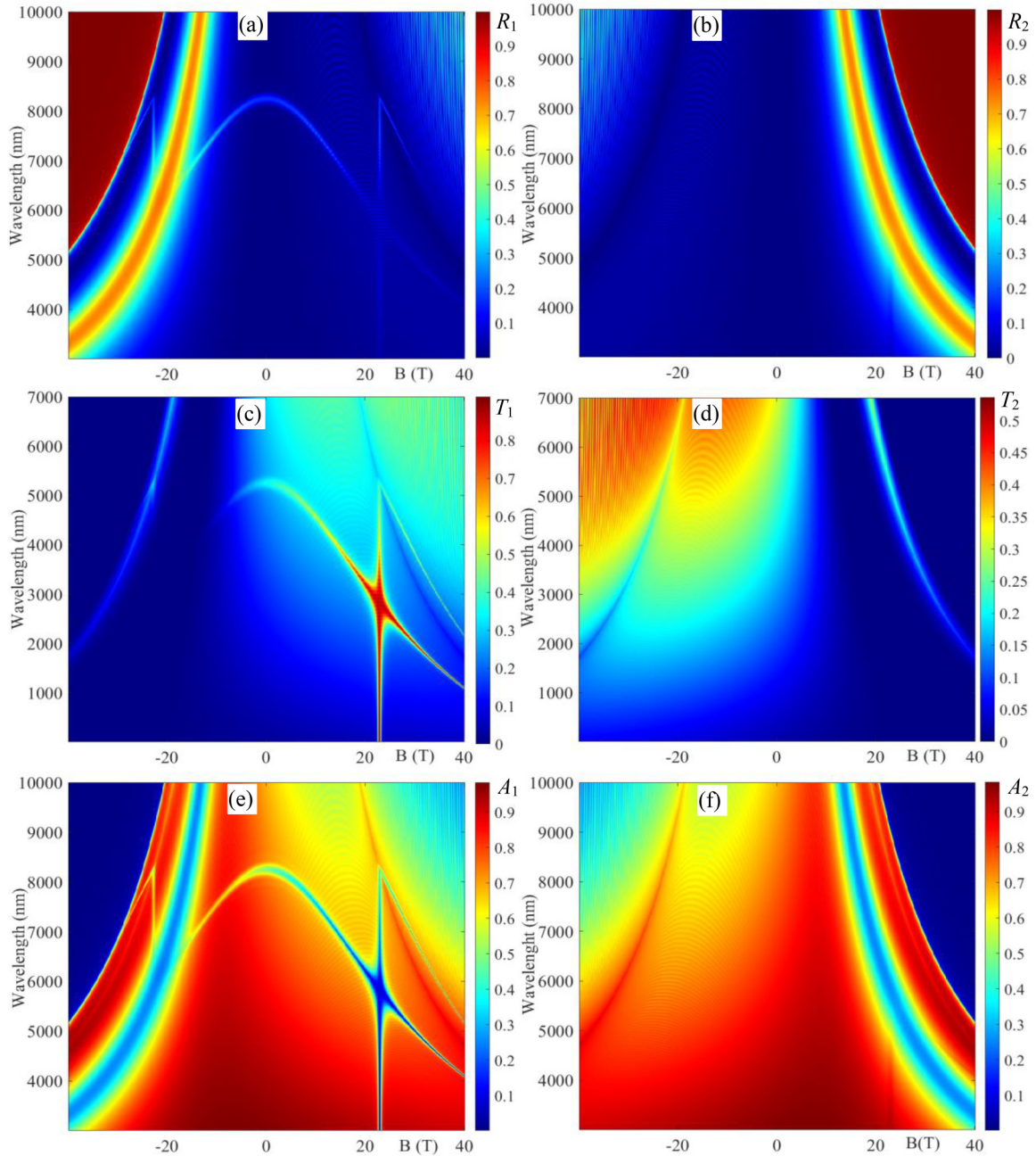
FIG. 7. The evolution of the spectra of (a, b) reflection R, (c, d) transmission T, and (e, f) absorption at the change of external magnetic field. The incident light has polarization coinciding with the first EP (left column) and with the second EP (right column). $p = 5500$ nm. The other parameters are the same as in Fig. 4.

III. CONCLUSIONS

In conclusion, we investigated the properties of dichroic CLCs being in an external static magnetic field directed along the helix axis. We have shown that in the case of the wavelength dependence of a magneto-optic activity parameter, new features appear in the optics of dichroic CLCs. First, we studied the behavior of the function $g(\lambda)$ and showed that it has two zeros and passes through a local maximum, and after the second zero it increases monotonically. We showed that in the point of the local maximum of $g(\lambda)$ we have a Dirac point, and moreover, in this Dirac point a new type of PBG

arises that differs from the basic PBG (i.e., the PBG that also exists in the absence of the external magnetic field). If the basic PBG is determined by the structure of the CLC, i.e., the chirality sign of the polarization of the incident diffracting light is determined only by the chirality sign of the CLC helix, then for the new one it is determined by the external magnetic field direction (i.e., on whether the directions of the external magnetic field and the incident light are parallel, or they are antiparallel). Near the second zero of $g(\lambda)$ a transmission band is formed for incident light with a certain polarization. And as for the second PBG, the chirality sign of the polarization of the

incident light for which this transmission band was formed is determined by the external magnetic field direction.

This system is nonreciprocal, and the nonreciprocity changes over a wide range, being observed both for reflection and transmittance and for absorption. The transformation of the region of the first (basic) PBG into a narrow window of MIT takes place with an increase in the pitch of the helix. With an increase of helix pitch at a certain value of the latter, instead of a narrow line of MIT, a broadband region of MIT is formed. With a further increase in the helix pitch a new Dirac point appears and a new MIT line appears. Then at g ⩾ ε, two from four wave vectors become complex at the absence of absorption and a new (the third) PBG appears.

Thus various types of PBGs, as well as MIT and MIA bands, can be formed at the Dirac points. As is well known, Dirac points in PCs also should be expected when the band gap closes and there aren't any PBGs in such types of Dirac points (see, also, [36]). The band gap in CLC closes when $\varepsilon_1 = \varepsilon_2 = \varepsilon$. Such a situation in CLC can arise, for example, in the presence of a frequency dispersion of local components of the dielectric permittivity tensor (by adding, for example, certain types of dye molecules or nanoparticles to CLC). Then it is possible that at some frequency ω_0 the intersection of the curves $y_1 = \frac{\omega}{c}\sqrt{\varepsilon_1(\omega)}$ and $y_2 = \frac{\omega}{c}\sqrt{\varepsilon_2(\omega)}$ is possible. If, at the same time, the condition $\frac{\omega}{c}\sqrt{\varepsilon_1(\omega_0)} = \frac{\omega}{c}\sqrt{\varepsilon_2(\omega_0)} = \frac{2\pi}{p}$ is also satisfied (by changing, for example, temperature), then the Dirac point will be formed at the frequency ω_0. In the absence of absorption, there will be no PBG in such a situation, although the medium itself is periodically inhomogeneous. In the presence of anisotropic absorption [and in a real situation the medium will indeed be anisotropically absorbing, since it will be difficult to ensure the simultaneous fulfillment of the conditions $\mathrm{Re}\varepsilon_1(\omega_0) = \mathrm{Re}\varepsilon_2(\omega_0)$ and $\mathrm{Im}\varepsilon_1(\omega_0) = \mathrm{Im}\varepsilon_2(\omega_0)$], we will have the Dirac point at which the PBG was formed.

We note once again that the case g = g(λ) differs substantially from the case g = const, which was considered in [27], which can by evidenced by a comparison of the results of this paper with the results obtained in [27].

Although most of our calculations were made at $B_{\mathrm{ext}} = 40$ T, the observed effects are also observed at much lower values of B_{ext}. At smaller values of B_{ext}, the frequency range of observation of these affects changes, and, moreover, in this case it is necessary to consider a wider wavelength region.

Let us now consider the influence of an external magnetic field on the CLC structure and the case of the presence of local dielectric anisotropy in CLCs. According to Meyer [37], the effect of an external magnetic field on the helix pitch in the lower order approximation is defined as

$$p(H) = p\left[1 + \frac{\chi_a^2 H_{\mathrm{ext}}^4\, p^4}{32(2\pi)^4 k_{22}^2} + \cdots \right], \qquad (6)$$

where χ_a is the anisotropy of magnetic susceptibility, k_{22} is the coefficient of elasticity, and H_{ext} is the external magnetic field. Since in our case $\hat{\mu}(z) = \hat{I}$, we can neglect the helix pitch change in the lowest order approximation.

Furthermore, as mentioned above, the magnetic field can also directly affect the local dielectric tensor components, which are a quadratic in the external field effect. Therefore,
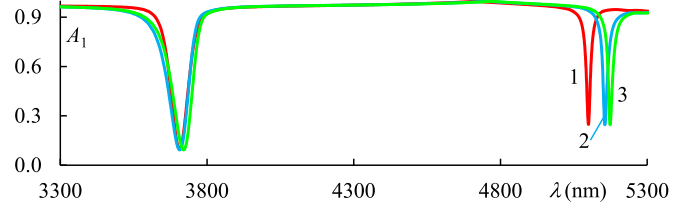
FIG. 8. The spectra of absorption. The incident light has polarization coinciding with the first EP: (1) $\alpha_1 = \alpha_2 = 0$; (2) $\alpha_1 = 4 \times 10^{-5}$, $\alpha_2 = 10^{-5}$; and (3) $\alpha_1 = 5 \times 10^{-5}$, $\alpha_2 = 2 \times 10^{-5}$. The other parameters are $\varepsilon_1 = 2.25$, $\varepsilon_2 = 2.25 + 0.1i$, $p = 4000$ nm, $d = 35p$, and $B_{\mathrm{ext}} = 40$ T.

according to [38], we can present the principal values of dielectric tensor components in the form of

$$\varepsilon_{1,2}(H_{\mathrm{ext}}) = \varepsilon_{1,2} + \alpha_{1,2}B_{\mathrm{ext}}^2, \qquad (7)$$

where $\alpha_{1,2}$ are some coefficients of proportionality. Figure 8 shows the spectra of absorption at different values of parameters α_1 and α_2. The simulation is made for a CLC with the parameters $\varepsilon_1 = 2.25$, $\varepsilon_2 = 2.25 + 0.1i$ $p = 4000$ nm. The CLC layer thickness is $d = 35p$ and $B_{\mathrm{ext}} = 40$ T. The following three cases are considered in our calculations, namely, (1) the CLC without local birefringence with $\alpha_1 = \alpha_2 = 0$; (2) $\alpha_1 = 4 \times 10^{-5}$, $\alpha_2 = 10^{-5}$; and finally, (3) $\alpha_1 = 5 \times 10^{-5}$, $\alpha_2 = 2 \times 10^{-5}$. As is seen from Fig. 8, the difference of $\alpha_{1,2}$ from zero brings the displacements of MIT bands. At the same time, this modeling shows that the main results and conclusions presented above depend on the local anisotropy, but not crucially, and they remain valid. Taking these into account leads to quantitative, but not qualitative, effects.

Finally, the soft-matter nature of CLCs and their response to external influences lead to easily tunable multifunctional devices that can find a variety of applications. They can be applied as tunable narrow-band or broadband filters and mirrors, a highly tunable wideband/narrow-band coherent perfect absorber, transmitters, ideal optical diodes, and other devices The results obtained can find application in the design of innovative polarized optoelectronic devices, in particular, as devices for chemical analysis, biomedical diagnostics, polarization selectors, polarization imaging, and spectroscopic measurements.

ACKNOWLEDGMENT

APPENDIX

The dependence of g on wavelength λ follows directly from the following considerations. First, the magnitude of Faraday rotation angle for an isotropic magnetoactive medium is given by the formula

$$\varphi = \frac{\pi d}{\lambda}(\sqrt{\varepsilon + \mathrm{g}} - \sqrt{\varepsilon - \mathrm{g}}), \qquad (A1)$$

where d is the transmission distance and ε is the dielectric permittivity. On the other hand, for the same magnitude of

rotation, experimenters use the formula $\varphi = VB_{\text{ext}}d$. Substituting $\varphi = VB_{\text{ext}}d$ into (A1) for g we will have

$$g = \frac{VB_{\text{ext}}\lambda}{\pi} \sqrt{\left| \varepsilon - \left(\frac{VB_{\text{ext}}\lambda}{2\pi} \right)^2 \right|}. \qquad \text{(A2)}$$

Now a little bit about the Verdet constant (for more on the constant Verdet, see the review article [39] and the references

cited therein, as well as [40,41]). It follows from [40,41] that for most magneto-optical media the Verdet constant undergoes changes mainly near some resonance lines, while in other regions of the spectrum it is constant. As shown in [41], two of these resonance lines are in the far-ultraviolet and near-infrared regions. So, in the near-ultraviolet, visible, and far-infrared regions the Verdet constant can be assumed to be constant, independent of wavelength.

[1] F. Bloch, Z. Physik **52**, 555 (1929).

[2] C. Zener, Proc. R. Soc. London A **145**, 523 (1934).

[3] M. Fleischhauer, A. Imamoglu, and J. P. Marangos, Rev. Mod. Phys. **77**, 633 (2005).

[4] M. S. Hur, J. S. Wurtele, and G. Shvets, Phys. Plasmas **10**, 3004 (2003).

[5] A. Lezama, S. Barreiro, and A. M. Akulshin, Phys. Rev. A **59**, 4732 (1999).

[6] R. Gad, J. G. Leopold, A. Fisher, F. R. Fredkin, and A. Ron, Phys. Rev. Lett. **108**, 155003 (2012).

[7] J. H. Yan, P. Liu, Z. Y. Lin, H. Wang, H. J. Chen, C. X. Wang, and G. W. Yang, Nat. Commun. **6**, 7042 (2015).

[8] D. Floess, M. Hentschel, T. Weiss, H. U. Habermeier, J. Jiao, S. G. Tikhodeev, and H. Giessen, Phys. Rev. X **7**, 021048 (2017).

[9] A. Christofi, Y. Kawaguchi, A. Alù, and A. B. Khanikaev, Opt. Lett. **43**, 1838 (2018).

[10] Z. Wu, J. Li, and Y. Wu, Phys. Rev. A **106**, 053525 (2022).

[11] M. N. Winchester, M. A. Norcia, J. R. K. Cline, and J. K. Thompson, Phys. Rev. Lett. **118**, 263601 (2017).

[12] A. Sommer, Physics **10**, 70 (2017).

[13] X. Zhang, C. L. Zou, L. Jiang, and H. X. Tang, Phys. Rev. Lett. **113**, 156401 (2014).

[14] G. H. Dong, D. Z. Xu, and P. Zhang, Phys. Rev. A **102**, 033717 (2020).

[15] K. Ullah, M. T. Naseem, and Ö. E. Müstecaplıoğlu, Phys. Rev. A **102**, 033721 (2020).

[16] A. H. Gevorgyan, Mol. Cryst. Liq. Cryst. **382**, 1 (2002).

[17] I. Bita and E. L. Thomas, J. Opt. Soc. Amer. A. **22**, 1199 (2005).

[18] I.-C. Khoo, *Liquid Crystals*, 2nd ed. (J. Wiley & Sons, Hoboken, NJ, 2007).

[19] A. H. Gevorgyan, Opt. Mat. **113**, 110807 (2021).

[20] A. H. Gevorgyan, S. S. Golik, and T. A. Gevorgyan, J. Magn. Magn. Mater. **537**, 168176 (2021).

[21] A. H. Gevorgyan, J. Mol. Liquids **335**, 116289 (2021).

[22] A. H. Gevorgyan and S. S. Golik, Opt. Las. Technol. **149**, 107810 (2022).

[23] A. H. Gevorgyan, J. Appl. Phys. **132**, 133101 (2022).

[24] P. K. Challa, V. Borshch, O. Parri, C. T. Imrie, S. N. Sprunt, J. T. Gleeson, O. D. Lavrentovich, and A. Jakli, Phys. Rev. E **89**, 060501(R) (2014).

[25] S. M. Salili, J. Xiang, H. Wang, Q. Li, D. A. Paterson, J. M. D. Storey, C. T. Imrie, O. D. Lavrentovich, S. N. Sprunt, J. T. Gleeson, and A. Jákli, Phys. Rev. E **94**, 042705 (2016).

[26] J. M. Caridad, C. Tserkezis, J. E. Santos, P. Plochocka, M. Venkatesan, J. M. D. Coey, N. A. Mortensen, G. L. J. A. Rikken, and V. Krstic, Phys. Rev. Lett. **126**, 177401 (2021).

[27] A. H. Gevorgyan, S. S. Golik, N. A. Vanyushkin, and I. M. Efimov, Optik **261**, 169208 (2022).

[28] A. H. Gevorgyan, Opt. Lett. **46**, 3616 (2021).

[29] A. H. Gevorgyan, J. Mol. Liq. **339**, 117276 (2021).

[30] A. H. Gevorgyan, Phys. Rev. E **105**, 014701 (2022).

[31] A. H. Gevorgyan, Phys. Lett. A **443**, 128222 (2022).

[32] A. H. Gevorgyan, N. A. Vanyushkin, I. M. Efimov, A. O. Kamenev, S. S. Golik, H. Gharagulyan, T. M. Sarukhanyan, Malek G. Daher, and K. B. Oganesyan, J. Opt. Soc. Am. B **40**, 1986 (2023).

[33] G. A. Vardanyan and A. A. Gevorgyan, Crystallogr. Rep. **42**, 663 (1997).

[34] A. H. Gevorgyan, S. S. Golik, Y. N. Kulchin, and N. A. Vanyushkin, Optik **247**, 167927 (2021).

[35] A. H. Gevorgyan, S. S. Golik, N. A. Vanyushkin, I. M. Efimov, M. S. Rafayelyan, H. Gharagulyan, T. M. Sarukhanyan, M. Z. Hautyunyan, and G. K. Matinyan, Materials **14**, 2172 (2021).

[36] W.-Y. He and C. T. Chan, Sci. Rep. **5**, 8186 (2015).

[37] R. B. Meyer, Appl. Phys. Lett. **12**, 281 (1968).

[38] A. K. Zvezdin and V. A. Kotov, *Modern Magnetooptics and Magnetooptical Materials* (CRC Press, Cleveland, OH, 1997), p. 404.

[39] D. Vojna, O. Slezák, A. Lucianetti, and T. Mocek, Appl. Sci. **9**, 3160 (2019).

[40] Y. Tamaru, H. Chen, A. Fuchimukai, H. Uehara, T. Miura, and R. Yasuhara, Opt. Mater. Exp. **11**, 814 (2021).

[41] O. Slezák, R. Yasuhara, D. Vojna, H. Furuse, A. Lucianetti, and T. Mocek, Opt. Mater. Exp. **9**, 2971 (2019).